ARTICLES

Tumour invasion and metastasis initiated by microRNA-10b in breast cancer

Li Ma[1], Julie Teruya-Feldstein[2] & Robert A. Weinberg[1]

MicroRNAs have been implicated in regulating diverse cellular pathways. Although there is emerging evidence that some microRNAs can function as oncogenes or tumour suppressors, the role of microRNAs in mediating cancer metastasis remains unexplored. Here we show, using a combination of mouse and human cells, that microRNA-10b (miR-10b) is highly expressed in metastatic breast cancer cells and positively regulates cell migration and invasion. Overexpression of miR-10b in otherwise non-metastatic breast tumours initiates robust invasion and metastasis. Expression of miR-10b is induced by the transcription factor Twist, which binds directly to the putative promoter of *mir-10b* (*MIRN10B*). The miR-10b induced by Twist proceeds to inhibit translation of the messenger RNA encoding homeobox D10, resulting in increased expression of a well-characterized pro-metastatic gene, *RHOC*. Significantly, the level of miR-10b expression in primary breast carcinomas correlates with clinical progression. These findings suggest the workings of an undescribed regulatory pathway, in which a pleiotropic transcription factor induces expression of a specific microRNA, which suppresses its direct target and in turn activates another pro-metastatic gene, leading to tumour cell invasion and metastasis.

Metastasis is a complex, multi-step process by which primary tumour cells invade adjacent tissue, enter the systemic circulation (intravasate), translocate through the vasculature, arrest in distant capillaries, extravasate into the surrounding tissue parenchyma, and finally proliferate from microscopic growths (micrometastases) into macroscopic secondary tumours[1]. In recent years, studies have been carried out to investigate the genes and gene products that drive the metastatic process. For instance, work in a number of laboratories has revealed several transcription factors that can program many of the cell-biological changes needed to execute the initial steps of the invasion–metastasis cascade[2–8].

Lately, it has become evident that, in addition to alterations in protein-encoding genes, abnormalities in non-coding genes can also contribute to cancer pathogenesis[9,10]. In particular, a class of small cellular RNAs, termed microRNAs (miRNAs), acting as agents of the RNA interference pathway, can lead to silencing of their cognate target genes, doing so either by cleaving mRNA molecules or by inhibiting their translation[11]. Indeed, miRNAs have been implicated in the regulation of a variety of cellular processes, including apoptosis[12], haematopoietic differentiation[13], metabolism[14], skin morphogenesis[15] and neural development[16].

More than 50% of annotated human miRNA genes are located in fragile chromosomal regions that are susceptible to amplification, deletion, or translocation during the course of tumour development[17]. Moreover, recent evidence indicates that some miRNAs can function either as oncogenes or tumour suppressors[10,18,19], and expression profiling analyses have revealed characteristic miRNA signatures in certain human cancers[9,20,21]. However, the precise parts played by the expressed miRNAs in specific steps of malignant progression, including metastasis, are still unknown. For these reasons, we undertook to associate specific miRNAs with specific stages of malignant progression, with the hope that such associations might provide insights into the causal mechanisms of cancer cell invasion and metastasis.

miR-10b is highly expressed in metastatic breast cancer cells

To identify miRNAs that regulate breast cancer metastasis, we selected candidate miRNAs on the basis of previously reported miRNA microarray profiling; these analyses had identified 29 miRNAs that are differentially expressed between primary breast carcinomas and normal mammary tissue, without regard to the eventual metastatic progression of these tumours[22]. We investigated the expression of these candidate miRNAs in a series of human mammary epithelial cells and tumour cell lines (Supplementary Table 1). Out of a total of eight selected miRNAs, three (miR-155, miR-9 and miR-10b) were found to be markedly upregulated in breast cancer cells when compared with either primary human mammary epithelial cells (HMECs) or with the spontaneously immortalized MCF-10A cells (Fig. 1a and Supplementary Table 1). Unlike miR-155 and miR-9, the expression of which was not specific to metastatic cells (Fig. 1a, b), miR-10b was highly expressed only in metastatic cancer cells. For example, the expression level of miR-10b was 50-fold higher in cells of the MDA-MB-231 line, which are capable of metastasizing, than in cells of the MCF-7 human breast cancer line, which have little if any metastatic powers (Fig. 1c). This correlation indicated that miR-10b might well have a causal role in breast cancer metastasis.

miR-10b positively regulates cell migration and invasion *in vitro*

We first performed *in vitro* loss-of-function analyses by silencing the miRNAs with antisense oligonucleotides[23]. We assessed the level of miRNA silencing by a reporter assay, in which the predicted miRNA binding site was cloned into the 3′ untranslated region (UTR) of a luciferase reporter gene[24]. We found that transfection of the antisense inhibitor for miR-9 or miR-10b in MDA-MB-231 cells caused a two- to threefold increase in the luciferase activity (Supplementary Fig. 1a, b), suggesting that each of the transfected antisense RNAs achieved a greater than 50% inhibition of the actions of its cognate miRNA. Although neither of these two antisense RNAs affected the motility of MDA-MB-231 cells (Fig. 1d), silencing of miR-10b led to a more

[1]Whitehead Institute for Biomedical Research and Department of Biology, Massachusetts Institute of Technology, Cambridge, Massachusetts 02142, USA. [2]Department of Pathology, Memorial Sloan-Kettering Cancer Center, New York, New York 10021, USA.

than tenfold reduction in the invasive properties of these cells, as gauged by an *in vitro* invasion assay in which miR-9 inhibition had only a marginal effect (Fig. 1e). This reduction was not due to impairment of cell viability (Supplementary Fig. 1c). Taken together, these observations suggested that miR-10b function is required for *in vitro* invasiveness but not for viability or motility of these metastatic cells.

To determine whether miR-10b overexpression would increase the basal levels of cell migration or invasion, we cloned the genomic sequence of the human *mir-10b* gene into a green fluorescent protein (GFP)-expressing, murine stem-cell retrovirus (MSCV)-derived vector[13]. We then used the resulting vector to express miR-10b in immortalized HMECs[25], and in the SUM149 cell line, a line of non-metastatic human breast cancer cells[26,27]. The miR-10b expression level was gauged by PCR with reverse transcription (RT–PCR; Fig. 1f).

In both cell lines, ectopic expression of miR-10b had no effect on their proliferation *in vitro* (Supplementary Fig. 1d, e), but did result in a four- to sixfold increase in cell motility and invasiveness (Fig. 1g, h). These results indicated that overexpression of miR-10b is sufficient to promote both migration and invasion *in vitro*.

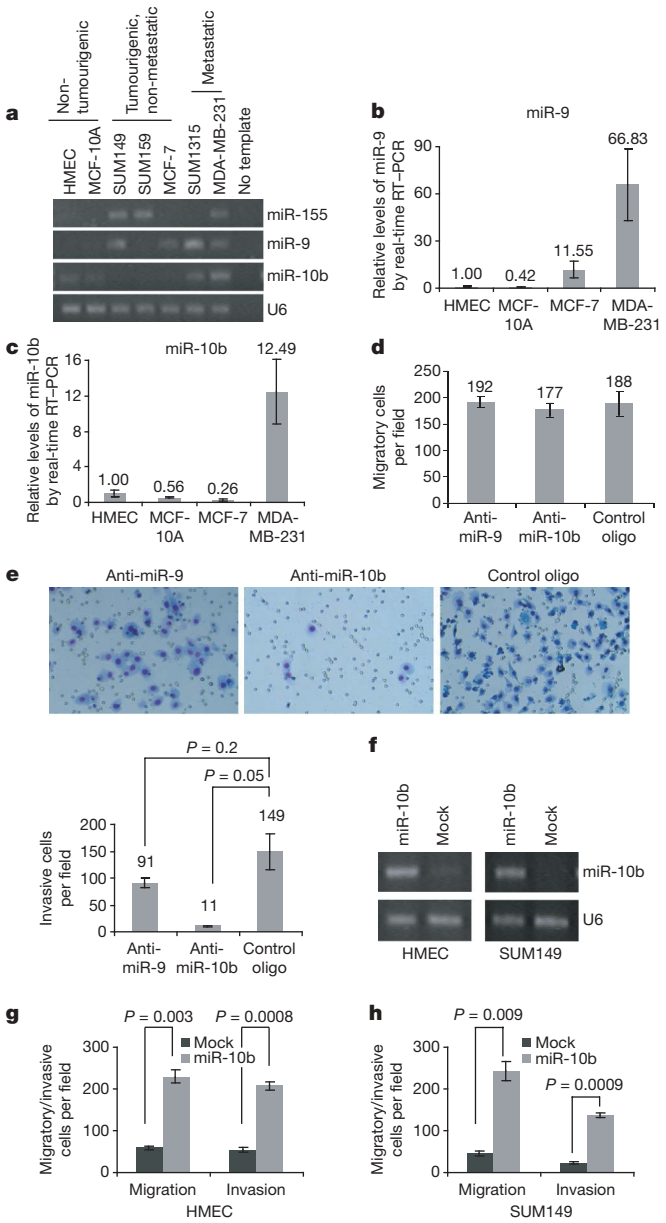

Figure 1 | miR-10b is highly expressed in metastatic breast cancer cells and positively regulates cell migration and invasion. a, RT–PCR of miR-155, miR-9 and miR-10b in a series of human mammary epithelial cells. **b**, **c**, Real-time RT–PCR of miR-9 (**b**) and miR-10b (**c**) in four different human mammary epithelial cells. **d**, **e**, Transwell migration assay (**d**) and Matrigel invasion assay (**e**) of MDA-MB-231 cells transfected with the inhibitor for miR-9 (anti-miR-9) or miR-10b (anti-miR-10b) (quantified below). Magnification in **e**, ×200. **f**, RT–PCR of miR-10b in HMECs and SUM149 cells infected with the miR-10b-expressing or empty vector. **g**, **h**, Transwell migration assay and Matrigel invasion assay of HMECs (**g**) and SUM149 cells (**h**) infected with the miR-10b-expressing or empty vector. A representative experiment is shown in triplicate along with s.e.m. in **b**–**e**, **g** and **h**.

miR-10b initiates tumour invasion *in vivo*

A key question was whether miR-10b could induce metastatic behaviours *in vivo*. To address this possibility, we overexpressed miR-10b in otherwise non-metastatic human breast cancer cells. To begin, we implanted miR-10b-transduced or mock-infected SUM149 cells into the mammary fat pads of NOD-SCID mice. The host mice displayed visible mammary tumours within two weeks after injection and became moribund at week 11 owing to primary tumour burden, at which point this experiment was terminated. Importantly, GFP expression was maintained in the tumour cells throughout this time period (Fig. 2a).

At 6 weeks post implantation, the control tumours and the miR-10b-overexpressing SUM149 tumours were of comparable size (Fig. 2b), indicating no effects of this miRNA on primary tumour formation. As anticipated, the control SUM149 tumours were strictly non-invasive, as shown by their confinement within fibrotic capsules (Fig. 2c, panels A, B). In stark contrast, the miR-10b-overexpressing SUM149 tumours displayed a massive desmoplastic reaction, with islands of epithelial cancer cells that had invaded the stroma (Fig. 2c, panels C, D). In addition, we observed apparent muscular and vascular invasion by the miR-10b-overexpressing tumour cells (Fig. 2c, panels E, F). Hence, ectopic expression of miR-10b could confer invasiveness on SUM149 cancer cells that were previously non-invasive *in vivo*.

To determine whether miR-10b expression in the primary tumours would also affect cell proliferation and tumour angiogenesis, we performed immunohistochemistry with the Ki-67 proliferation marker and the MECA-32 endothelial cell marker. We found that the distribution, but not the total number, of Ki-67$^+$ cells in the miR-10b-overexpressing SUM149 tumours was distinct from that seen in the control tumours: in the miR-10b-expressing tumours, large necrotic centres were apparent that lacked proliferating cells, whereas the invasion fronts were enriched in Ki-67$^+$ cells and were highly vascularized (Fig. 2d, panel E–H, and Fig. 2e, f); this contrasted with the appearance of the control tumours, which exhibited an essentially even distribution of Ki-67$^+$ cells (interspersed with Ki-67$^-$ cells) and poor vascularization (Fig. 2d, panel A–D, and Fig. 2e, f). Furthermore, in contrast to the control tumours, the vessels associated with the invasion fronts of the miR-10b-overexpressing tumours were seen not only in the stroma (peritumoural), but also within the epithelial tumour masses (intratumoural, Fig. 2g). Hence, the invasion fronts of miR-10b-overexpressing tumours exhibited very high levels of both cell proliferation and angiogenesis.

At later times, those mice injected with miR-10b-overexpressing cells carried larger tumour burdens ($P = 0.03$, Fig. 2b). We concluded that the enhanced tumour growth of these miR-10b-overexpressing cells was likely to be a consequence rather than a cause of their invasiveness, because (1) the substantial stromal invasion by the miR-10b-expressing cells preceded by several weeks the observed differences in overall tumour growth rates, and (2) the miR-10b-transduced cells and their control counterparts proliferated at similar rates *in vitro* (Supplementary Fig. 1d, e) and *in vivo* (as gauged by overall levels of Ki-67, Fig. 2d, e). Thus, we speculate that vascularization might be a rate-limiting determinant of overall tumour growth, and that increased invasiveness might afford the miR-10b-overexpressing cells better access to the vasculature.

miR-10b initiates distant metastasis

We asked whether expression of miR-10b would also result in distant metastasis. As early as week 6, haematoxylin and eosin staining revealed the presence of miR-10b-overexpressing SUM149 cells in the primary tumour-associated vessels (Fig. 2c, panel F). Immunohistochemical analyses further revealed significant numbers of hyperproliferative Ki-67$^+$ tumour cells in the lumina of some of the vessels associated with the miR-10b-overexpressing tumours (Fig. 3a). In contrast, no significant evidence of intravasating or intravasated cancer cells was found in the control tumours.

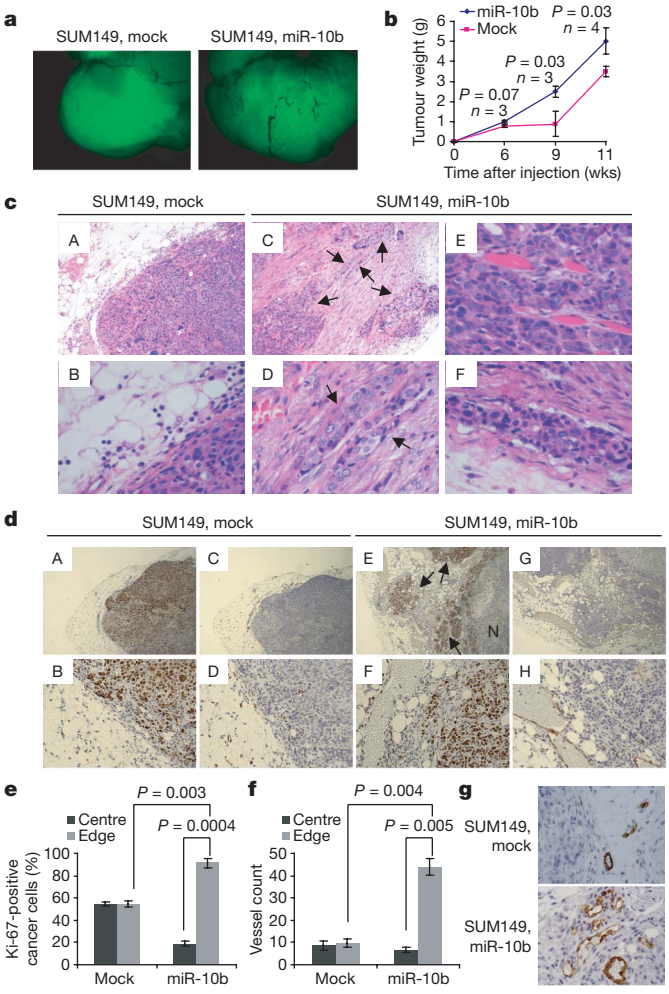

Figure 2 | miR-10b induces tumour invasion. **a**, GFP imaging of the SUM149 primary tumours at week 11 after orthotopic injection of NOD-SCID mice. Magnification, ×8. **b**, Growth curves of primary mammary tumours formed by SUM149 cells infected with the miR-10b-expressing or empty vector. Each data point represents the mean ± s.e.m. of 3–4 mice. **c**, Haematoxylin and eosin (H&E)-stained sections of primary mammary tumours formed by SUM149 cells infected with the miR-10b-expressing or empty vector, at week 6 after orthotopic transplantation. Arrows in panels C and D indicate areas of stromal invasion. Panels E and F demonstrate muscular invasion and vascular invasion, respectively. Magnification: panels A and C, ×100; panels B and D–F, ×400. **d**, Ki-67- (panels A, B, E, F) and MECA-32- (panels C, D, G, H) stained sections of primary mammary tumours formed by SUM149 cells infected with the miR-10b-expressing or empty vector, at week 6 after orthotopic transplantation. Arrows in panel E indicate areas of invasion. N, necrosis. Magnification: panels A, C, E and G, ×40; panels B, D, F and H, ×200. **e**, **f**, Quantification of Ki-67 staining (percentage of Ki-67$^+$ carcinoma cells among total carcinoma cells; **e**) and vessels (using MECA-32-stained sections; **f**) at the centre and the edge of the SUM149 tumours. $n = 3$ mice at 6 weeks after implantation. Error bars in **e** and **f** indicate s.e.m. **g**, Prominent intratumoural vessels are associated with the invasion front of miR-10b-overexpressing tumours, as demonstrated by MECA-32 staining of primary mammary tumours formed by SUM149 cells infected with the miR-10b-expressing or empty vector, at week 6 after orthotopic transplantation. Magnification, ×400.

We also examined other tissues for the presence of disseminated tumour cells. At week 6 after implantation, we observed occasional single GFP$^+$ cells in a few regions of the lung cryosections, indicating relatively early dissemination of the miR-10b-overexpressing cells from primary tumours; the lungs of mice that carried control tumours lacked such GFP$^+$ cells (Supplementary Fig. 2). At 9 weeks after implantation, the lungs from mice implanted with miR-10b-overexpressing SUM149 cells exhibited clusters of dense hyperchromatic cells that were positive for cytokeratins, as demonstrated by staining with AE1/AE3 (a cocktail of two distinct anti-cytokeratin monoclonal antibodies, Fig. 3b). On average, we found ~1 micrometastasis per 5-μm section (Fig. 3c, left panel). At week 11, there was a further increase in the number of such micrometastatic clusters (~4 micrometastases per section, Fig. 3c, right panel). In the lungs of hosts bearing control SUM149 tumours, however, the only AE1/AE3-positive cells were normal bronchial epithelial cells (Fig. 3b).

The ability of ectopically expressed miR-10b to elicit metastasis was also examined in the SUM159 cell line—a second line of human breast cancer cells. These cells are invasive but non-metastatic[27], allowing us to determine whether these cells too would respond to miR-10b by acquiring metastatic potential. In contrast to the SUM149 cells described above, control SUM159 cells exhibited a high level of motility and invasiveness *in vitro* (data not shown). Moreover, the xenograft mammary tumours formed by the control SUM159 cells displayed local invasion (data not shown). Importantly, no metastases were found in 10 mice that had been transplanted with mock-infected SUM159 cells (Fig. 3d, f). Strikingly, however, 8 out of 10 mice that had received orthotopic transplantation of miR-10b-overexpressing SUM159 cells exhibited numerous lung metastases, which were readily detectable both by GFP fluorescence and by histological analysis (Fig. 3d, f). Furthermore, 30% of these mice (3/10) developed macroscopic peritoneal metastases (0.5–2 cm in diameter, Fig. 3e, f). Taken together, these observations indicate that ectopic miR-10b expression can drive tumour invasion and metastasis in otherwise non-metastatic breast tumours, thereby acting as a potent pro-metastatic agent.

miR-10b is directly regulated by the transcription factor Twist

We undertook to determine how miR-10b expression is regulated. The observation that miR-10b is highly expressed in metastatic breast cancer cells indicated that the gene encoding this miRNA might be the target of certain transcription factors that are activated specifically in metastatic cells. Of note, recent studies have demonstrated that several transcription factors previously known as master regulators of embryogenesis, are highly expressed in metastatic cells and seem to have causal roles in tumour metastasis, ostensibly by inducing epithelial–mesenchymal transitions (EMTs) in cancer cells[2–8]; this process is thought to contribute to the invasiveness and dissemination of epithelial tumour cells[28]. These various observations led us to ask whether any of these EMT-inducing factors might function to activate miR-10b expression.

We first assessed miR-10b expression in the four lines of mouse mammary tumour cells that had been used in the identification of *Twist* as a metastasis-promoting gene[6]. We discovered that the level of miR-10b correlated with the known metastatic potentials of these cell types, with the lowest expression level in 67NR cells, which are unable to intravasate from the primary tumour, whereas the highest expression level was seen in 4T1 cells, which are capable of generating macroscopic metastases (Fig. 4a, b). This closely paralleled the expression pattern of Twist in these cell lines[6], indicating that miR-10b expression might well be upregulated by this transcription factor. We therefore expressed either Twist1 (also known as Twist) or, as a control, a second EMT-inducing transcription factor—snail (SNAI1)—in the non-tumourigenic, immortalized HMECs, which had been found to express a low level of miR-10b (Fig. 1f). In contrast

to the behaviour of SNAI1, which reduced miR-10b expression by 57%, ectopic expression of Twist1 led to a 4.5-fold increase in the level of this miRNA in these HMECs (Fig. 4c, d).

We next performed chromatin immunoprecipitation (ChIP) assays to determine whether TWIST1 controls miR-10b expression by binding directly to the *mir-10b* gene. This basic helix–loop–helix transcription factor has been shown to bind to E-box sequences (CANNTG) present in the genes that it regulates[29,30]. We examined the 4-kb genomic sequence upstream of the human *mir-10b* stem-loop and identified two conserved E-boxes, at −313 bp (E-box 1) and −2,422 bp (E-box 2), respectively (Fig. 4e). In addition, the putative promoter of human *mir-10b* spans between −111 bp and −460 bp[31], which encompasses E-box 1, the most proximal E-box. We designed two PCR amplicons to assay for the presence of these two putative binding sites in chromatin immunoprecipitates. The experiments revealed that TWIST1 bound to E-box 1, but not to E-box 2 (Fig. 4e). Thus, TWIST1 specifically binds to the putative promoter of *mir-10b*, providing strong evidence that miR-10b can be directly regulated by this transcription factor.

Although miR-10b does not seem to be essential for cell motility in highly metastatic cancer cells (Fig. 1d), we asked nonetheless whether this miRNA is required for Twist1-induced migration and invasion in otherwise poorly motile cells. To this end, we introduced the antisense oligonucleotide for miR-10b into Twist1-overexpressing HMECs. In accord with a previous report[6], overexpression of Twist1 led to a strong increase in the motility and invasiveness of

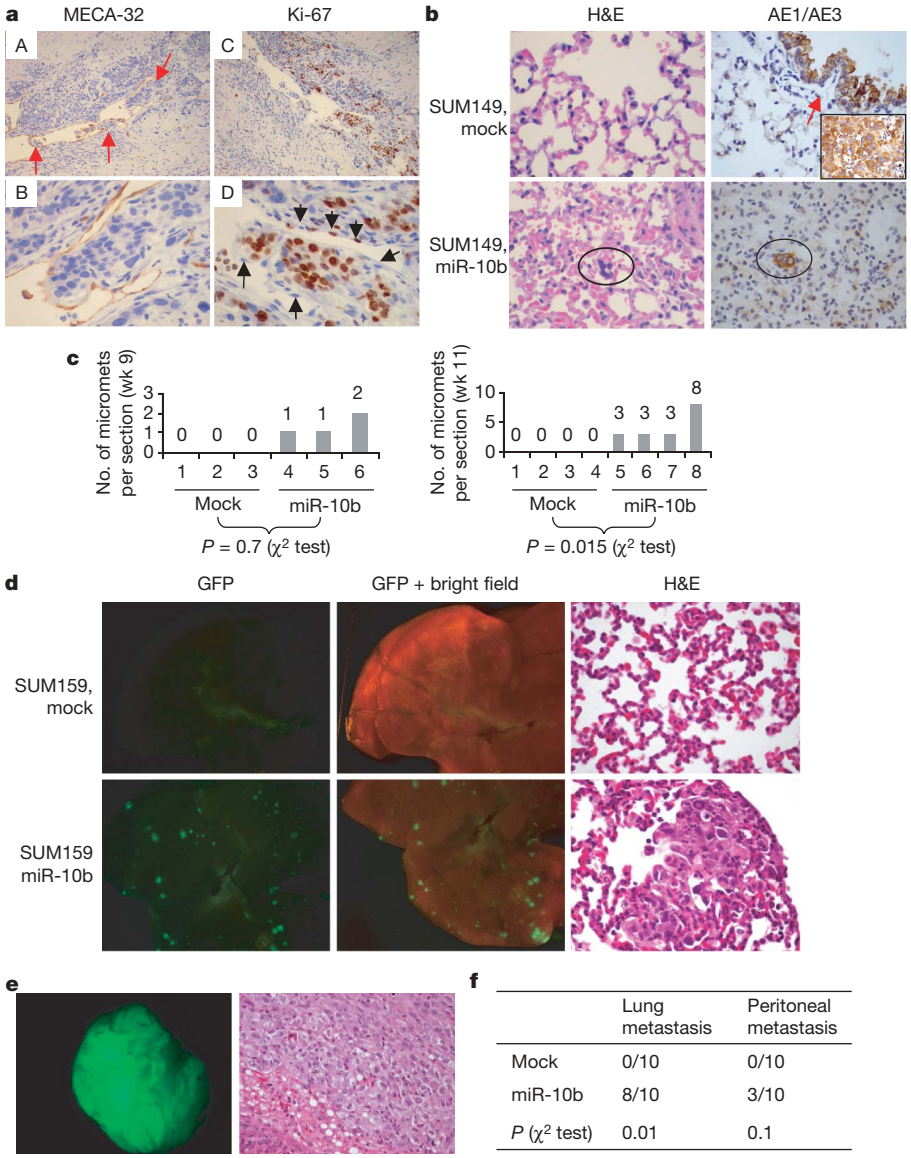

f

	Lung metastasis	Peritoneal metastasis
Mock	0/10	0/10
miR-10b	8/10	3/10
P (χ^2 test)	0.01	0.1

Figure 3 | miR-10b induces distant metastasis. a, MECA-32- and Ki-67-stained sections of a primary mammary tumour formed by miR-10b-transduced SUM149 cells, at week 6 after orthotopic transplantation. Red arrows in panel A indicate tumour cells within a vessel, and black arrows in panel D indicate endothelial cells. Magnification: panels A and C, ×100; panels B and D: ×400. **b**, H&E- and AE1/AE3-stained sections of lungs isolated from mice that received orthotopic injection of miR-10b-transduced or mock-infected SUM149 cells, at week 9 after transplantation. Circles indicate clusters of metastatic cells. The arrow indicates normal bronchial epithelium. Inset, AE1/AE3 staining of a SUM149 primary tumour. Magnification, ×600. **c**, Numbers of lung micrometastases (micromets) per section in individual mice that received orthotopic injection of miR-10b-transduced or mock-infected SUM149 cells, at week 9 (left panel) and week 11 (right panel) after transplantation, respectively. **d**, Bright field, GFP imaging, and H&E staining of lungs isolated from mice that received orthotopic injection of miR-10b-transduced or mock-infected SUM159 cells, at week 11 after transplantation. Magnification, ×8 for bright field and GFP imaging; ×600 for H&E staining. **e**, GFP imaging and H&E staining of a macroscopic peritoneal metastasis in a mouse that received orthotopic injection of miR-10b-transduced SUM159 cells, at week 11 after transplantation. Magnification, ×8 for GFP imaging; ×400 for H&E staining. **f**, Incidence of lung metastasis and macroscopic peritoneal metastasis in mice that received orthotopic injection of miR-10b-transduced or mock-infected SUM159 cells.

these cells (Fig. 4f). Strikingly, miR-10b inhibition consistently led to a fivefold reduction in the motility and invasiveness of Twist1-overexpressing HMECs (Fig. 4f). Whereas Twist1 is capable, on its own, of inducing an EMT[6], miR-10b is not (data not shown). Instead, it seems to be essential to one element of the multi-component, Twist1-induced EMT program—increased cell motility and invasiveness.

HOXD10 is a direct and functional target of miR-10b

To understand the mechanisms by which miR-10b induces tumour invasion and metastasis, we used several computational methods to help identify miR-10b targets in humans. Among the approximately 100 targets predicted by both the TargetScan[32] and PicTar[33] search programs, two genes—homeobox D10 (*HOXD10*) and *RB1CC1* (also named *FIP200*)—were previously implicated in suppression of cell migration and/or invasion. *HOXD10* was of particular interest, because its expression has been found to be progressively lost in breast tumours showing increasing degrees of malignancy[34,35]. More importantly, restored expression of HOXD10 in MDA-MB-231 cells has been found to impair migration and invasion *in vitro* as well as tumour progression *in vivo*[35]. The *HOXD10*-encoded mRNA contains a 3′ UTR element that is partially complementary to miR-10b and carries the identical sequence in the human, mouse and rat mRNA orthologues (Fig. 5a).

Although miR-10b overexpression did not cause degradation of *HOXD10* mRNA (Fig. 5b), it did, however, reduce the activity of a luciferase reporter gene fused to the wild-type *HOXD10* 3′ UTR (48% reduction, $P = 0.003$, Fig. 5c), indicating that miR-10b targets *HOXD10* through translational inhibition. The action of miR-10b on *HOXD10* depends on the presence of a single miR-10b cognate binding site within the 3′ UTR, because the activity of a luciferase reporter that carries a mutant *HOXD10* 3′ UTR—with substitution of four nucleotides within the miR-10b binding site (Fig. 5a)—was not reduced by expression of miR-10b (Fig. 5c). In support of these results, we observed a clear reduction in the level of the endogenous HOXD10 protein in miR-10b-overexpressing cells (tenfold and threefold reduction in HMECs and SUM149 cells, respectively, Fig. 5d).

Others have demonstrated that HOXD10 represses expression of genes that are involved in cell migration and extracellular matrix remodelling, including RHOC, α3 integrin, matrix metalloproteinase-14, and urokinase-type plasminogen activator receptor[36]. Among these, RHOC has been identified as an especially important player

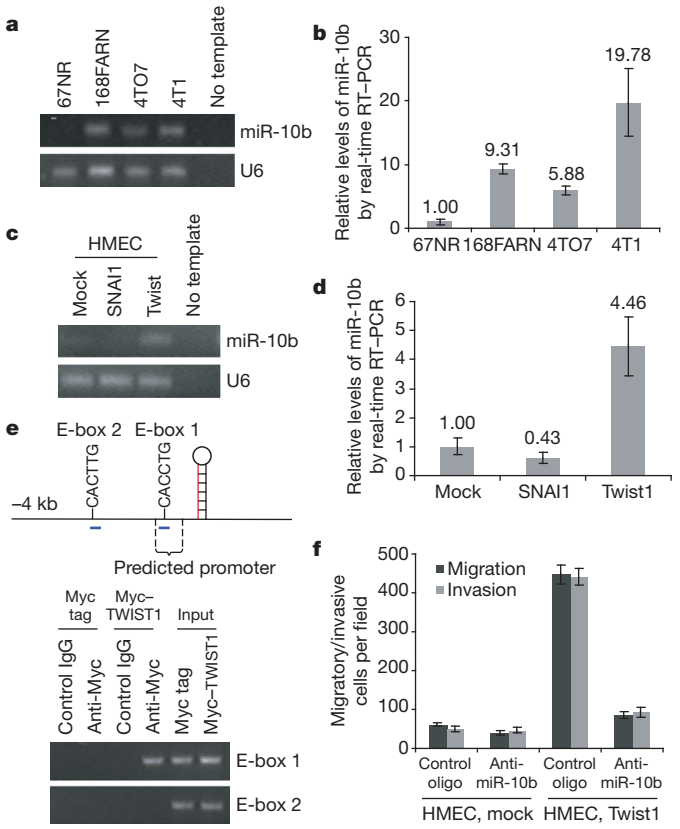

Figure 4 | miR-10b is regulated by Twist. **a**, **b**, RT–PCR (**a**) and real-time RT–PCR (**b**) of miR-10b in 67NR, 168FARN, 4TO7 and 4T1 cells. **c**, **d**, RT–PCR (**c**) and real-time RT–PCR (**d**) of miR-10b in HMECs transduced by SNAI1, Twist1 or the empty vector. **e**, Upper panel, human *mir-10b* genomic locus. The two short blue lines represent two PCR amplicons. Lower panel, ChIP assay in HEK293T cells transfected with a vector expressing Myc–TWIST1 or the Myc tag alone. PCR was performed with primers specific for human *mir-10b* E-box 1 and E-box 2, respectively. **f**, Transwell migration assay and Matrigel invasion assay of Twist1-transduced or mock-infected HMECs that were transfected with the inhibitor for miR-10b or the control oligonucleotide. A representative experiment is shown in triplicate along with s.e.m. in **b**, **d** and **f**.

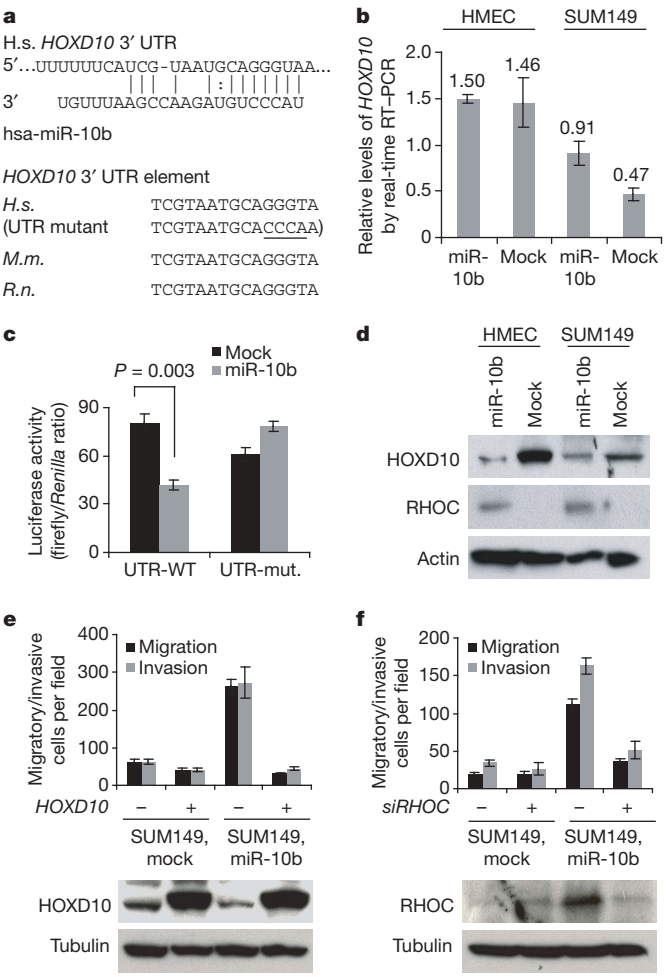

Figure 5 | miR-10b suppresses HOXD10, leading to induction of RHOC. **a**, Upper panel, predicted duplex formation between human *HOXD10* 3′ UTR and miR-10b. Lower panel, sequence of the miR-10b binding site within the *HOXD10* 3′ UTR of human (*H.s.*), and within the *HoxD10* 3′ UTR of mouse (*M.m.*), and rat (*R.n.*). **b**, Real-time RT–PCR of *HOXD10* in HMECs and SUM149 cells infected with the miR-10b-expressing or empty vector. Data were normalized to the level of *GAPDH* mRNA. **c**, Luciferase activity of wild-type (UTR-WT) or mutant (UTR-mut.) *HOXD10* 3′ UTR reporter gene in SUM149 cells infected with the miR-10b-expressing or empty vector. **d**, Immunoblotting of HOXD10 and RHOC in HMECs and SUM149 cells infected with the miR-10b-expressing or empty vector. **e**, **f**, Upper panel, transwell migration assay and Matrigel invasion assay of miR-10b-transduced or mock-infected SUM149 cells with transient transfection of *HOXD10* (**e**) or *RHOC* siRNA (**f**). Lower panel, immunoblotting of HOXD10 (**e**) or RHOC (**f**). A representative experiment is shown in triplicate along with s.e.m. in **b**, **c**, **e** and **f**.

in metastasis[37,38], and its expression correlates with metastatic spread of various types of carcinomas[39–41]. Indeed, we found that miR-10b-transduced cells exhibited robust expression of RHOC protein, whereas RHOC expression in the control cells was barely detectable (Fig. 5d).

We next ascertained whether reduction of HOXD10 levels might provide an explanation for the induction of cell motility and invasiveness observed following miR-10b overexpression. We overexpressed miR-10b in SUM149 cells together with a construct expressing HOXD10 constitutively; this construct encodes the entire HOXD10 coding sequence but lacks the 3′ UTR of HOXD10-encoding mRNA, yielding an mRNA that is resistant to miR-10b-mediated inhibition of translation. Strikingly, the resulting constitutive expression of HOXD10 completely abrogated miR-10b-induced cell motility and invasiveness (Fig. 5e), without affecting the proliferation or viability of these cells (data not shown), suggesting that this *HOX* gene is indeed a functionally important target of miR-10b. Furthermore, transfection of *RHOC* siRNA (small-interfering RNA), which caused a > 90% reduction in the level of the RHOC protein (Fig. 5f), led to a strong but not complete suppression of miR-10b-induced cell migration (by 81%) and invasion (by 87%, Fig. 5f). Hence, RHOC seems to be a key downstream effector of miR-10b.

miR-10b expression is elevated in metastatic breast tumours

Paradoxically, a recent microarray study reported that miR-10b is among the miRNAs found to be downregulated in primary breast tumours (independent of their clinical aggressiveness) compared with normal breast tissue[22]. To address this apparent paradox and determine whether miR-10b expression correlates with clinical outcome in patients, we measured its levels in primary tumour samples from 23 breast cancer patients. When compared with normal breast tissue, miR-10b expression level was lower in all of the breast carcinomas from metastasis-free patients (5/5). In contrast, 50% of the metastasis-positive patients (9/18) had elevated miR-10b levels in their primary tumours ($P = 0.03$, Fig. 6a).

These results are in consonance with the expression pattern of miR-10b in cultured human mammary cells (Fig. 1c). In addition, we observed that ectopic miR-10b expression in non-tumourigenic, immortalized EpH4 mouse mammary epithelial cells[42] did not transform them to a tumourigenic state, whereas overexpression of Ras indeed enabled their tumourigenic growth (data not shown). Collectively, our findings indicate that miR-10b plays a part specifically in the metastatic process but not in primary tumour formation.

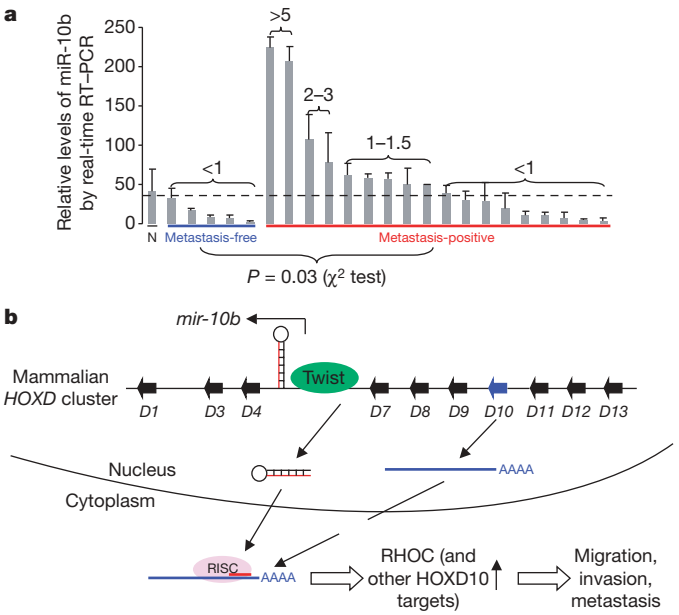

Figure 6 | miR-10b expression level is associated with the metastasis outcome in breast cancer patients. a, Real-time RT–PCR of miR-10b in 23 primary breast tumours from patients with indicated status of metastasis. N, normal breast tissue. Error bars indicate s.e.m. of triplicate experiments. The numbers above the columns indicate fold increase relative to normal tissue. **b**, Model for the regulation and function of miR-10b in cancer metastasis. RISC, RNA-induced silencing complex.

Discussion

The present work has led to the identification of a Twist-induced miRNA (miR-10b) that inhibits synthesis of the HOXD10 protein, permitting the expression of the pro-metastatic gene product, RHOC; this favours, in turn, cancer cell migration and invasion (Fig. 6b). Importantly, overexpression of this miRNA in otherwise non-metastatic breast cancer cells enables them to acquire invasive and metastatic behaviour. Conversely, silencing of miR-10b inhibits Twist-mediated cell migration and invasion. It remains to be seen whether miR-10b inhibition in highly malignant cells will reverse the metastatic phenotype *in vivo*. Such analysis is hampered at present by the lack of an experimental strategy for stably silencing miRNAs over extended periods of time.

Of particular interest, the *mir-10b* gene is located within the *HOXD* gene cluster (Fig. 6b). In fact, a number of *HOX* genes have been predicted to be targets of miRNA regulation, both in vertebrates[32] and in flies[43], and some of these associations have been validated experimentally: (1) miR-196, which has near perfect complementarity with the *HOXB8* mRNA 3′UTR region, downregulates *HOXB8* expression through cleavage of this mRNA[44]; and (2) miR-iab-4-5p downregulates ultrabithorax (UBX, a *Drosophila* HOX protein), leading to a homeotic phenotype in flies[45]. Accordingly, miR-10b represents a third 'HOX miRNA' that regulates expression of a *HOX* gene within the same *HOX* gene cluster that carries its encoding gene. This indicates that miR-10b is also likely to be involved in regulating certain steps of embryogenesis in which HOXD10 is known to participate. In addition, a close relative of miR-10b, miR-10a (the gene for which is located within the *HOXB* gene cluster), has been recently reported to target *HOXA1* (ref. 46), a gene that plays an oncogenic role in human mammary carcinoma cells[47], indicating that miR-10a might have an opposite rather than similar function in breast cancer.

In silico analyses predict that yet other mRNAs are direct targets of miR-10b-mediated silencing. Because the invasion–metastasis cascade involves a number of distinct steps[1], it is therefore possible that miR-10b regulates additional targets that are involved in several of these steps. A future challenge will be to identify the entire complement of miRNAs and their mRNA targets to elucidate more fully the contributions of these miRNAs to high-grade malignancy.

METHODS SUMMARY

Quantification of miRNAs was performed by real-time RT–PCR. Activity of miRNAs was measured by a luciferase reporter assay. Silencing of miRNAs was done by transfection of a chemically modified antisense oligonucleotide that was complementary to the endogenous miRNA being targeted. Ectopic expression of miR-10b was achieved by retroviral infection. Cell motility and invasiveness were gauged by transwell migration assay and Matrigel invasion assay, respectively. Chromatin immunoprecipitation was performed with a ChIP assay kit, followed by PCR with primers specific for *mir-10b*. Metastatic activity was assayed by mammary fat pad injection of cancer cells into NOD-SCID female mice. GFP imaging, histological analysis and cytokeratin immunohistochemistry were used to detect distant metastasis. Human materials were obtained from the Memorial Sloan-Kettering Cancer Center along with pathology reports and radiological reviews.

Full Methods and any associated references are available in the online version of the paper at www.nature.com/nature.

Received 29 June; accepted 16 August 2007.
Published online 26 September 2007.

1. Fidler, I. J. The pathogenesis of cancer metastasis: the 'seed and soil' hypothesis revisited. *Nature Rev. Cancer* **3**, 453–458 (2003).

2. Batlle, E. *et al.* The transcription factor snail is a repressor of *E-cadherin* gene expression in epithelial tumour cells. *Nature Cell Biol.* **2,** 84–89 (2000).
3. Cano, A. *et al.* The transcription factor snail controls epithelial–mesenchymal transitions by repressing *E-cadherin* expression. *Nature Cell Biol.* **2,** 76–83 (2000).
4. Comijn, J. *et al.* The two-handed E box binding zinc finger protein SIP1 downregulates *E-cadherin* and induces invasion. *Mol. Cell* **7,** 1267–1278 (2001).
5. Bolos, V. *et al.* The transcription factor Slug represses *E-cadherin* expression and induces epithelial to mesenchymal transitions: a comparison with Snail and E47 repressors. *J. Cell Sci.* **116,** 499–511 (2003).
6. Yang, J. *et al.* Twist, a master regulator of morphogenesis, plays an essential role in tumor metastasis. *Cell* **117,** 927–939 (2004).
7. Hartwell, K. A. *et al.* The Spemann organizer gene, *Goosecoid*, promotes tumor metastasis. *Proc. Natl Acad. Sci. USA* **103,** 18969–18974 (2006).
8. Mani, S. A. *et al.* Mesenchyme Forkhead 1 (*FOXC2*) plays a key role in metastasis and is associated with aggressive basal-like breast cancers. *Proc. Natl Acad. Sci. USA* **104,** 10069–10074 (2007).
9. Calin, G. A. & Croce, C. M. MicroRNA signatures in human cancers. *Nature Rev. Cancer* **6,** 857–866 (2006).
10. Esquela-Kerscher, A. & Slack, F. J. Oncomirs — microRNAs with a role in cancer. *Nature Rev. Cancer* **6,** 259–269 (2006).
11. Bartel, D. P. MicroRNAs: genomics, biogenesis, mechanism, and function. *Cell* **116,** 281–297 (2004).
12. Brennecke, J., Hipfner, D. R., Stark, A., Russell, R. B. & Cohen, S. M. *bantam* encodes a developmentally regulated microRNA that controls cell proliferation and regulates the proapoptotic gene *hid* in *Drosophila. Cell* **113,** 25–36 (2003).
13. Chen, C. Z., Li, L., Lodish, H. F. & Bartel, D. P. MicroRNAs modulate hematopoietic lineage differentiation. *Science* **303,** 83–86 (2004).
14. Poy, M. N. *et al.* A pancreatic islet-specific microRNA regulates insulin secretion. *Nature* **432,** 226–230 (2004).
15. Yi, R. *et al.* Morphogenesis in skin is governed by discrete sets of differentially expressed microRNAs. *Nature Genet.* **38,** 356–362 (2006).
16. Schratt, G. M. *et al.* A brain-specific microRNA regulates dendritic spine development. *Nature* **439,** 283–289 (2006).
17. Calin, G. A. *et al.* Human microRNA genes are frequently located at fragile sites and genomic regions involved in cancers. *Proc. Natl Acad. Sci. USA* **101,** 2999–3004 (2004).
18. He, L. *et al.* A microRNA polycistron as a potential human oncogene. *Nature* **435,** 828–833 (2005).
19. Johnson, S. M. *et al.* RAS is regulated by the let-7 microRNA family. *Cell* **120,** 635–647 (2005).
20. Lu, J. *et al.* MicroRNA expression profiles classify human cancers. *Nature* **435,** 834–838 (2005).
21. Roldo, C. *et al.* MicroRNA expression abnormalities in pancreatic endocrine and acinar tumors are associated with distinctive pathologic features and clinical behavior. *J. Clin. Oncol.* **24,** 4677–4684 (2006).
22. Iorio, M. V. *et al.* MicroRNA gene expression deregulation in human breast cancer. *Cancer Res.* **65,** 7065–7070 (2005).
23. Meister, G., Landthaler, M., Dorsett, Y. & Tuschl, T. Sequence-specific inhibition of microRNA- and siRNA-induced RNA silencing. *RNA* **10,** 544–550 (2004).
24. Cheng, A. M., Byrom, M. W., Shelton, J. & Ford, L. P. Antisense inhibition of human miRNAs and indications for an involvement of miRNA in cell growth and apoptosis. *Nucleic Acids Res.* **33,** 1290–1297 (2005).
25. Elenbaas, B. *et al.* Human breast cancer cells generated by oncogenic transformation of primary mammary epithelial cells. *Genes Dev.* **15,** 50–65 (2001).
26. Ethier, S. P., Mahacek, M. L., Gullick, W. J., Frank, T. S. & Weber, B. L. Differential isolation of normal luminal mammary epithelial cells and breast cancer cells from primary and metastatic sites using selective media. *Cancer Res.* **53,** 627–635 (1993).
27. Kuperwasser, C. *et al.* A mouse model of human breast cancer metastasis to human bone. *Cancer Res.* **65,** 6130–6138 (2005).
28. Thiery, J. P. Epithelial–mesenchymal transitions in tumour progression. *Nature Rev. Cancer* **2,** 442–454 (2002).
29. Cripps, R. M. *et al.* The myogenic regulatory gene *Mef2* is a direct target for transcriptional activation by Twist during *Drosophila* myogenesis. *Genes Dev.* **12,** 422–434 (1998).
30. Cheng, G. Z. *et al.* Twist transcriptionally up-regulates *AKT2* in breast cancer cells leading to increased migration, invasion, and resistance to paclitaxel. *Cancer Res.* **67,** 1979–1987 (2007).
31. Zhou, X., Ruan, J., Wang, G. & Zhang, W. Characterization and identification of microRNA core promoters in four model species. *PLoS Comput. Biol.* **3,** e37 (2007).
32. Lewis, B. P., Shih, I. H., Jones-Rhoades, M. W., Bartel, D. P. & Burge, C. B. Prediction of mammalian microRNA targets. *Cell* **115,** 787–798 (2003).
33. Krek, A. *et al.* Combinatorial microRNA target predictions. *Nature Genet.* **37,** 495–500 (2005).
34. Makiyama, K. *et al.* Aberrant expression of *HOX* genes in human invasive breast carcinoma. *Oncol. Rep.* **13,** 673–679 (2005).
35. Carrio, M., Arderiu, G., Myers, C. & Boudreau, N. J. Homeobox D10 induces phenotypic reversion of breast tumor cells in a three-dimensional culture model. *Cancer Res.* **65,** 7177–7185 (2005).
36. Myers, C., Charboneau, A., Cheung, I., Hanks, D. & Boudreau, N. Sustained expression of homeobox D10 inhibits angiogenesis. *Am. J. Pathol.* **161,** 2099–2109 (2002).
37. Clark, E. A., Golub, T. R., Lander, E. S. & Hynes, R. O. Genomic analysis of metastasis reveals an essential role for RhoC. *Nature* **406,** 532–535 (2000).
38. Hakem, A. *et al.* RhoC is dispensable for embryogenesis and tumor initiation but essential for metastasis. *Genes Dev.* **19,** 1974–1979 (2005).
39. Kleer, C. G. *et al.* RhoC GTPase expression as a potential marker of lymph node metastasis in squamous cell carcinomas of the head and neck. *Clin. Cancer Res.* **12,** 4485–4490 (2006).
40. Kondo, T. *et al.* Expression of *RhoC* is associated with metastasis of gastric carcinomas. *Pathobiology* **71,** 19–25 (2004).
41. Wang, W. *et al.* Overexpression of the *RhoC* gene correlates with invasion and metastasis of hepatocellular carcinoma *Chinese J. Oncol.* (Zhonghua Zhong Liu Za Zhi.), **26,** 279–282 (2004).
42. Reichmann, E. *et al.* Activation of an inducible c-FosER fusion protein causes loss of epithelial polarity and triggers epithelial–fibroblastoid cell conversion. *Cell* **71,** 1103–1116 (1992).
43. Enright, A. J. *et al.* MicroRNA targets in *Drosophila. Genome Biol.* **5,** R1 (2003).
44. Yekta, S., Shih, I. H. & Bartel, D. P. MicroRNA-directed cleavage of *HOXB8* mRNA. *Science* **304,** 594–596 (2004).
45. Ronshaugen, M., Biemar, F., Piel, J., Levine, M. & Lai, E. C. The *Drosophila* microRNA iab-4 causes a dominant homeotic transformation of halteres to wings. *Genes Dev.* **19,** 2947–2952 (2005).
46. Garzon, R. *et al.* MicroRNA fingerprints during human megakaryocytopoiesis. *Proc. Natl Acad. Sci. USA* **103,** 5078–5083 (2006).
47. Zhang, X. *et al.* Human growth hormone-regulated *HOXA1* is a human mammary epithelial oncogene. *J. Biol. Chem.* **278,** 7580–7590 (2003).

Supplementary Information is linked to the online version of the paper at www.nature.com/nature.

Acknowledgements We thank D. Bartel, H. Lodish, P. Rao, B. Zhou, S. Mani, J. Yang, S. Ethier, C. Largman and L.-H. Wang for reagents and advice; F. Reinhardt for assistance with animal experiments; the Histology Core Laboratory at MIT and MSKCC for assistance with sectioning and immunohistochemistry; C. Mayr, C. Scheel, S. McAllister, I. Ben-Porath, Y. Sun and Y. Luo for critical reading of the manuscript; and members of the Weinberg Laboratory for useful discussions. L.M. is a Susan G. Komen Fellow of the Life Sciences Research Foundation. J.T.-F. is supported by the MSKCC Cancer Core Grant. R.A.W. is an American Cancer Society Research Professor and a Daniel K. Ludwig Cancer Research Professor. This research is supported by an NIH grant (R.A.W.) and the Ludwig Center for Molecular Oncology at MIT.

Author Contributions L.M. conceived the project. R.A.W. supervised research. L.M. designed and performed experiments. L.M. and J.T.-F. collected and analysed data. All authors contributed to the preparation of the manuscript.

Author Information Reprints and permissions information is available at www.nature.com/reprints. The authors declare no competing financial interests. Correspondence and requests for materials should be addressed to R.A.W. (weinberg@wi.mit.edu).

METHODS

Cell lines. The human mammary epithelial cells (HMECs, primary and immortalized) were described previously[25]. The MCF-10A, MCF-7, MDA-MB-231, and HEK293T cell lines were from ATCC and cultured under conditions provided by the manufacturer. Cell lines SUM149, SUM159 and SUM1315 were provided by S. Ethier and grown as described (http://www.asterand.com/Asterand/BIOREPOSITORY/AsterandSUMcelllineInstructions.pdf). 67NR, 168FARN, 4TO7 and 4T1 cell lines were cultured as previously described[6].

Constructs. The MDH1-PGK-GFP 2.0 vector was described previously[13]. The binding site for miR-9 or miR-10b, and the *HOXD10* 3′ UTR sequence were cloned into the pMIR-REPORT luciferase construct[24] (Ambion). The human *HOXD10* complementary DNA was a gift from C. Largman. Myc-tagged TWIST1 was provided by L.-H. Wang. The mutant construct of *HOXD10* 3′ UTR was generated using a QuikChange Site-Directed Mutagenesis Kit (Stratagene).

RNA isolation and miRNA detection. Total RNA from cultured cells, with efficient recovery of small RNAs, was isolated using the mirVana miRNA Isolation Kit (Ambion). Detection of the mature form of miRNAs was performed using the mirVana qRT–PCR miRNA Detection Kit and qRT–PCR Primer Sets, according to the manufacturer's instructions (Ambion). The U6 small nuclear RNA was used as an internal control.

miRNA gene cloning and ectopic expression. The human miRNA gene was PCR-amplified from normal genomic DNA and cloned into the MDH1-PGK-GFP 2.0 retroviral vector. The production of amphotropic viruses and infection of target cells were described previously[48]. The GFP^+ cells accounted for over 90% of infected cells, as determined by fluorescence-activated cell sorting (FACS) analysis.

Oligonucleotide transfection. The miRIDIAN microRNA inhibitors (Dharmacon) are single-stranded chemically enhanced oligonucleotides designed to inhibit the endogenous miRNAs. SMARTpool RHOC (Dharmacon) represents four pooled SMART-selected siRNA duplexes that target *RHOC* (the sense sequences are: GAAAGAAGCUGGUGAUCGUUU; GAACUAUAUUGCGGACAUUUU; GGACAUGGCGAACCGGAUCUU; CUACGUCCCUACUGUCUUUUU). Cells were transfected with 200 nM of the indicated oligonucleotide using the Oligofectamine reagent (Invitrogen). Forty-eight hours after transfection, cells were plated for migration and invasion assays, or harvested for the luciferase reporter assay.

***In vitro* migration and invasion assay.** For transwell migration assays, 2.5×10^4 to 5×10^4 cells were plated in the top chamber with the non-coated membrane (24-well insert; pore size, 8 μm; BD Biosciences). For invasion assays, 1.25×10^5 cells were plated in the top chamber with Matrigel-coated membrane (24-well insert; pore size, 8 μm; BD Biosciences). In both assays, cells were plated in medium without serum or growth factors, and medium supplemented with growth factors (for HMECs) or serum (for all other cells) was used as a chemoattractant in the lower chamber. The cells were incubated for 24 h and cells that did not migrate or invade through the pores were removed by a cotton swab. Cells on the lower surface of the membrane were stained with the Diff-Quick Staining Set (Dade) and counted.

Surgery, necropsy, histopathology and immunohistochemistry. Six-week-old female NOD-SCID mice (from Jackson Laboratory) were used for surgery. Mice were anaesthetized with 2,2,2-tribromoethanol. The skin was incised and tumour cells (1×10^6) in 25 μl growth medium were injected into the mammary fat pad. Each group consisted of 10 mice: for recipients of SUM149 cells, 3–4 mice per group were euthanized at each of the three time points (week 6, 9 and 11 post transplantation); for recipients of SUM159 cells, mice were euthanized when the tumours reached 2 cm in diameter, and thus the metastases by SUM159 cells were evaluated with mice carrying primary tumours of the same size, at the same time point (week 11–12 post transplantation). The mammary tumours were removed and weighed. The tumours, lungs, livers, spleens and macroscopic metastases were analysed under a dissecting microscope equipped with bright field and GFP fluorescence imaging. Tissue samples were fixed in 10% buffered formalin for 12 h, followed by a wash with PBS and transfer to 70% ethanol, and then embedded in paraffin, sectioned and stained with haematoxylin and eosin. The immunohistochemistry detection using anti-Ki-67 (1:50, Pharmingen) and anti-MECA-32 (1:50, from University of Iowa)-antibodies was performed on paraffin sections, using a BioGenex i6000 automated stainer in the Histology Core Laboratory at MIT. The immunohistochemistry detection using anti-cytokeratin antibodies AE1/AE3 (1:800, BioGenex) was performed on paraffin sections in the Histology Core Laboratory at MSKCC.

Luciferase reporter assay. Cells of 50% confluence in 24-well plates were transfected using Fugene6 (Roche). Firefly luciferase reporter gene construct (200 ng) and 1 ng of the pRL-SV40 *Renilla* luciferase construct (for normalization) were cotransfected per well. Cell extracts were prepared 24–48 h after transfection, and the luciferase activity was measured using the Dual-Luciferase Reporter Assay System (Promega).

Chromatin immunoprecipitation (ChIP) assay. ChIP was performed with HEK293T cells transfected with a vector expressing Myc–TWIST1 or the Myc tag alone, using a ChIP assay kit (Upstate), according to the manufacturer's instructions, Protein–DNA complexes were precipitated with control IgG or anti-Myc antibody (Covance). PCR was performed with primers specific for human *mir-10b*.

Immunoblotting. Cells were harvested in RIPA lysis buffer (150 mM NaCl, 10 mM Tris, pH 7.5, 1% NP40, 1% deoxycholate, 0.1% SDS, protease inhibitor cocktail (Roche)). Proteins from total cell lysates were resolved by the NuPAGE 4–12% Bis-Tris gradient gel (Invitrogen), transferred to the PVDF membrane, blocked in 5% non-fat milk in PBS/Tween-20, and blotted with the antibodies for HOXD10 (1:200, Santa Cruz), RHOC (1:200, Santa Cruz), α-tubulin (1:10,000, Abcam), and β-actin (1:10,000, Abcam).

Patient study. Patient samples of primary breast carcinoma were consecutively ascertained at MSKCC between 1993 and 2005. Use of tissue samples was approved with an Institutional Review Board (IRB) Waiver and approved by the Human Tissue Utilization Committee (HTUC). All breast carcinoma samples were obtained at the time of mastectomy. Of the 18 patients diagnosed with metastases, all had lymph node metastases with documented pathology from total mastectomies with axillary node dissections. In addition, metastatic spread to the contralateral breast (3 occurences), chest wall (3), pleural fluid (1), and ovary (1), was documented by histological review of biopsies taken at the time of mastectomy and/or subsequent surgeries; diffuse osseous metastases and adnexal mass (1) and spinal metastases (4) were documented by radiological reviews including bone scans, CT scans, PET scans, and/or MRI scans. Total RNA, with efficient recovery of small RNAs, was isolated from four 20-μm sections from formalin-fixed, paraffin-embedded tissue blocks, using the RecoverAll Total Nucleic Acid Isolation Kit (Ambion). Quantification of miR-10b by real-time RT–PCR was performed as previously mentioned.

Statistical Analysis. Data are presented as mean ± s.e.m. Student's *t* test (two-tailed) was used to compare two groups ($P < 0.05$ was considered significant) unless otherwise indicated (χ^2 test).

48. Stewart, S. A. *et al.* Lentivirus-delivered stable gene silencing by RNAi in primary cells. *RNA* **9**, 493–501 (2003).

CORRIGENDUM

doi:10.1038/nature07253

Genome analysis of the platypus reveals unique signatures of evolution

Wesley C. Warren, LaDeana W. Hillier, Jennifer A. Marshall Graves, Ewan Birney, Chris P. Ponting, Frank Grützner, Katherine Belov, Webb Miller, Laura Clarke, Asif T. Chinwalla, Shiaw-Pyng Yang, Andreas Heger, Devin P. Locke, Pat Miethke, Paul D. Waters, Frédéric Veyrunes, Lucinda Fulton, Bob Fulton, Tina Graves, John Wallis, Xose S. Puente, Carlos López-Otín, Gonzalo R. Ordóñez, Evan E. Eichler, Lin Chen, Ze Cheng, Janine E. Deakin, Amber Alsop, Katherine Thompson, Patrick Kirby, Anthony T. Papenfuss, Matthew J. Wakefield, Tsviya Olender, Doron Lancet, Gavin A. Huttley, Arian F. A. Smit, Andrew Pask, Peter Temple-Smith, Mark A. Batzer, Jerilyn A. Walker, Miriam K. Konkel, Robert S. Harris, Camilla M. Whittington, Emily S. W. Wong, Neil J. Gemmell, Emmanuel Buschiazzo, Iris M. Vargas Jentzsch, Angelika Merkel, Juergen Schmitz, Anja Zemann, Gennady Churakov, Jan Ole Kriegs, Juergen Brosius, Elizabeth P. Murchison, Ravi Sachidanandam, Carly Smith, Gregory J. Hannon, Enkhjargal Tsend-Ayush, Daniel McMillan, Rosalind Attenborough, Willem Rens, Malcolm Ferguson-Smith, Christophe M. Lefèvre, Julie A. Sharp, Kevin R. Nicholas, David A. Ray, Michael Kube, Richard Reinhardt, Thomas H. Pringle, James Taylor, Russell C. Jones, Brett Nixon, Jean-Louis Dacheux, Hitoshi Niwa, Yoko Sekita, Xiaoqiu Huang, Alexander Stark, Pouya Kheradpour, Manolis Kellis, Paul Flicek, Yuan Chen, Caleb Webber, Ross Hardison, Joanne Nelson, Kym Hallsworth-Pepin, Kim Delehaunty, Chris Markovic, Pat Minx, Yucheng Feng, Colin Kremitzki, Makedonka Mitreva, Jarret Glasscock, Todd Wylie, Patricia Wohldmann, Prathapan Thiru, Michael N. Nhan, Craig S. Pohl, Scott M. Smith, Shunfeng Hou, Mikhail Nefedov[1], Pieter J. de Jong[1], Marilyn B. Renfree, Elaine R. Mardis & Richard K. Wilson

[1]Children's Hospital Oakland Research Institute, Bruce Lyon Research Building, 747 52nd Street, Oakland, California 94609, USA.

Nature 453, 175–183 (2008)

In this Article, Mikhail Nefedov and Pieter J. de Jong were omitted from the author list.

ERRATUM

doi:10.1038/nature07316

Tumour invasion and metastasis initiated by microRNA-10b in breast cancer

Li Ma, Julie Teruya-Feldstein & Robert A. Weinberg

Nature 449, 682–688 (2007)

In Fig. 4e of this Article, the two E-box sequences were inadvertently exchanged. E-box 1, which is near the stem-loop (at −313 bp), should be CACTTG instead of CACCTG, and E-box 2 (at −2,422 bp), which is distal to the stem-loop, should be CACCTG instead of CACTTG.